Journal of
Chemical Engineering & Process Technology

Trivedi et al., J Chem Eng Process Technol 2015, 6:5
DOI: 10.4172/2157-7048.1000249

Research Article Open Access

Physical, Thermal and Spectroscopic Characterization of Biofield Treated *p*-Chloro-*m*-cresol

Mahendra Kumar Trivedi[1], Alice Branton[1], Dahryn Trivedi[1], Gopal Nayak[1], Ragini Singh[2] and Snehasis Jana[2]*

[1]*Trivedi Global Inc., 10624 S Eastern Avenue Suite A-969, Henderson, NV 89052, USA*
[2]*Trivedi Science Research Laboratory Pvt. Ltd., Hall-A, Chinar Mega Mall, Chinar Fortune City, Hoshangabad Rd., Bhopal, Madhya Pradesh, India*

Abstract

p-Chloro-m-cresol(PCMC) is widely used in pharmaceutical industries as biocide and preservative. However, it faces the problems of solubility in water and photo degradation. The aim of present study was to evaluate the impact of biofield treatment on physical, thermal and spectral properties of PCMC. For this study, PCMC sample was divided into two groups i.e., one served as treated and other as control. The treated group received Mr. Trivedi's biofield treatment and both control and treated samples of PCMC were characterized using X-ray diffraction (XRD), surface area analyser, differential scanning calorimetry (DSC), thermogravimetric analysis (TGA), Fourier transform infrared (FT-IR), ultraviolet-visible (UV-Vis) spectroscopy and gas chromatography–mass spectrometry (GC-MS). The XRD result showed a 12.7% increase in crystallite size in treated samples along with increase in peak intensity as compared to control. Moreover, surface area analysis showed a 49.36% increase in surface area of treated PCMC sample as compared to control. The thermal analysis showed significant decrease (25.94%) in the latent heat of fusion in treated sample as compared to control. However, no change was found in other parameters like melting temperature, onset temperature of degradation, and T_{max} (temperature at which maximum weight loss occur). The FT-IR spectroscopy did not show any significant change in treated PCMC sample as compared to control. Although, the UV-Vis spectra of treated samples showed characteristic absorption peaks at 206 and 280 nm, the peak at 280 nm was not found in control sample. The control sample showed another absorbance peak at 247 nm. GC-MS data revealed that carbon isotopic ratio ($\delta^{13}C$) was changed up to 204% while $\delta^{18}O$ and $\delta^{37}Cl$ isotopic ratio were significantly changed up to 142% in treated samples as compared to control. These findings suggest that biofield treatment has significantly altered the physical, thermal and spectroscopic properties, which can affect the solubility and stability of *p*-chloro-*m*-cresol and make it more useful as a pharmaceutical ingredient.

Keywords: Biofield treatment; *p*-chloro-*m*-cresol; X-ray diffraction; Surface area analysis; Differential scanning calorimetry; Thermogravimetric analysis; Fourier transform infrared spectroscopy; Ultraviolet-visible spectroscopy; Gas chromatography-mass spectrometry

Introduction

p-Chloro-*m*-cresol (PCMC) which is also known as chlorocresol (Figure 1), is used as an external germicide and bactericide agent. It has bactericidal activity against Gram positive and Gram negative organisms, along with yeasts, moulds and spores [1]. It is also used as preservative for various pharmaceutical preparations like cosmetics, lotions, tanning agents, and topical corticosteroids [2,3]. Other than that, it is also used in glues, paints and varnishes, and leather goods [4]. Moreover, it is used widely in eye drops, injections, shampoos and emulsions due to its disinfectant and antifungal properties [5]. Its antiseptic property makes it suitable for use in heparin solutions, and in various creams for skin care and dermatological care [6,7]. Apart from that, it is reported as potent activator of Ca^{2+} release mediated by ruthenium red/caffeine-sensitive Ca^{2+} release channel in skeletal muscle sarcoplasmic reticulum [8].

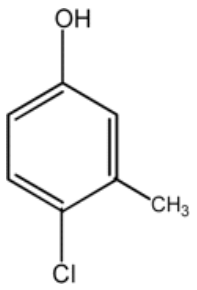

Figure 1: Chemical structure of *p*-chloro-*m*-cresol.

Although PCMC is widely used in pharmaceutical preparations but its effectiveness was reduced due to some problems related to solubility and stability [9]. Hence some alternative strategies are needed which can modulate the physicochemical properties of PCMC. The biofield treatment is an alternative strategy which is known to alter the properties of living and non-living materials. Biofield treatment is considered under complementary and alternative medicine and based on subtle energy field called biofield energy [10-12]. The human beings are infused with this precise form of energy. It is the scientifically defined as biologically produced electromagnetic and subtle energy field that provides regulatory and communication functions within the organism [13-15]. The health of living organisms can be inflected by balancing this energy from environment through natural exchange process [16]. Thus, human has the ability to harness the energy from environment or universe and can transmit into any living or non-living object(s) around the Universe. The objects always receive the energy and responding into useful way, that is called biofield energy and the process is known as biofield treatment. Mr. Trivedi's unique biofield treatment (The Trivedi Effect®) is known to alter the growth and yield properties of plants in the field of agriculture [17-19]. The effect of biofield treatment was also reported on plant's growth, anatomical characteristics and adaptation in biotechnology field [20,21] and

***Corresponding author:** Snehasis Jana, Trivedi Science Research Laboratory Pvt. Ltd., Hall-A, Chinar Mega Mall, Chinar Fortune City, Hoshangabad Rd., Bhopal-462 026, Madhya Pradesh, India, Tel: 91-755-6660006; E-mail: publication@trivedisrl.com

Received September 01, 2015; **Accepted** September 28, 2015; **Published** October 03, 2015

Citation: Trivedi MK, Branton A, Trivedi D, Nayak G, Singh R, et al. (2015) Physical, Thermal and Spectroscopic Characterization of Biofield Treated *p*-Chloro-*m*-cresol. J Chem Eng Process Technol 6: 249. doi:10.4172/2157-7048.1000249

phenotypic characters of microorganisms in field of microbiology [22-24]. Besides that, the impact of biofield treatment was also reported on physical, thermal and spectral properties of various metals and organic compounds [25-27]. Hence, the current study was designed to evaluate the impact of biofield treatment on physical, thermal and spectroscopic properties of PCMC.

Materials and Methods

Sample preparation

P-chloro-m-cresol (PCMC) was procured from Sisco Research Laboratories, India. The sample was divided into two parts; one was kept as a control while other was coded as treated sample. The treatment sample in sealed pack was handed over to Mr. Trivedi for biofield treatment under standard laboratory conditions. Mr. Trivedi provided the treatment through his energy transmission process to the treated group without touching the sample. The biofield treated sample was returned in the similarly sealed condition. Both control and treated samples were characterized using XRD, surface area analyser, DSC, TGA, FT-IR, UV-Vis and GC-MS spectroscopic techniques.

X-ray diffraction (XRD) study

XRD analysis was carried out on Phillips, Holland PW 1710 X-ray diffractometer system. The X-ray generator was equipped with a copper anode with nickel filter operating at 35 kV and 20 mA. The radiation of wavelength used by the XRD system was 1.54056 Å. The XRD spectra were acquired over the 2θ range of 10°-99.99° at 0.02° interval with a measurement time of 0.5 second per 2θ intervals. The data obtained were in the form of a chart of 2θ *vs.* intensity and a detailed table containing peak intensity counts, d value (Å), peak width (θ°), and relative intensity (%) etc.

The average size of crystallite (G) was calculated from the Scherrer equation with the method based on the width of the diffraction patterns obtained in the X-ray reflected crystalline region.

$G=k\lambda/(bCos\theta)$

Where, k is the equipment constant (0.94), λ is the X-ray wavelength (0.154 nm), B in radians is the full-width at half of the peaks and θ the corresponding Bragg angle.

However, percent change in crystallite size was calculated using the following equation:

Percent change in crystallite size$=[(G_t-G_c)/G_c]\times 100$

Where, G_c and G_t are crystallite size of control and treated powder samples respectively.

Surface area analysis

The surface area was measured by the Brunauer–Emmett–Teller (BET) surface area analyser, Smart SORB 90. Percent changes in surface area were calculated using following equation:

$$\%\text{ change in Surface area} = \frac{[S_{Treated} - S_{Control}]}{S_{Control}} \times 100$$

Where, $S_{Control}$ and $S_{Treated}$ are the surface area of control and treated samples respectively.

Differential scanning calorimetry (DSC) study

For studies related to melting temperature and latent heat of fusion of PCMC, Differential Scanning Calorimeter (DSC) of Perkin Elmer/ Pyris-1 was used. The DSC curves were recorded under air atmosphere (5 mL/min) and a heating rate of 10°C/min in the temperature range of 50°C to 350°C. An empty pan sealed with cover pan was used as a reference sample. Melting temperature and latent heat of fusion were obtained from the DSC curve.

Percent change in latent heat of fusion was calculated using following equations to observe the difference in thermal properties of treated PCMC sample as compared to control:

$$\%\text{ change in Latent heat of fusion} = \frac{[\Delta H_{Treated} - \Delta H_{Control}]}{\Delta H_{Control}} \times 100$$

Where, $\Delta H_{Control}$ and $\Delta H_{Treated}$ are the latent heat of fusion of control and treated samples, respectively.

Thermogravimetric analysis/Derivative thermogravimetry (TGA/DTG)

Thermal stability of control and treated sample of PCMC was analysed by using Mettler Toledo simultaneous Thermogravimetric analyser (TGA/DTG). The samples were heated from room temperature to 400°C with a heating rate of 5°C/min under air atmosphere. From TGA curve, onset temperature T_{onset} (temperature at which sample start losing weight) and from DTG curve, T_{max} (temperature at which sample lost its maximum weight) were observed.

Percent change in onset peak temperature was calculated using following equation:

% change in onset peak temperature $T_{onset}=[(T_{onset,\ treated}-T_{onset,\ control})/T_{onset,\ control}]\times 100$

Where, $T_{onset,\ control}$ and $T_{onset,\ treated}$ are onset peak temperature in control and treated sample, respectively.

Spectroscopic studies

For determination of FT-IR and UV-Vis spectroscopic characters, the treated sample was divided into two groups i.e., T1 and T2. Both treated groups were analysed for their spectral characteristics using FT-IR and UV-Vis spectroscopy as compared to control PCMC sample. For GC-MS analysis, the treated sample was divided into four groups i.e., T1, T2, T3, and T4 and all treated groups were analysed along with control sample for isotopic abundance ratio of carbon, oxygen and chlorine.

FT-IR spectroscopic characterization

The samples were crushed into fine powder for analysis. The powdered sample was mixed in spectroscopic grade KBr in an agate mortar and pressed into pellets with a hydraulic press. FT-IR spectra were recorded on Shimadzu's Fourier transforms infrared spectrometer (Japan). The samples were prepared by grinding the dry blended powders of control and treated PCMC with powdered KBr, and then compressed to form discs. FT-IR spectra were generated by the absorption of electromagnetic radiation in the frequency range 4000-400 cm^{-1}. The FT-IR spectroscopic analysis of PCMC (control, T1 and T2) were carried out to evaluate the impact of biofield treatment at atomic and molecular level like bond strength, stability, and rigidity of structure etc. [28].

UV-Vis spectroscopic analysis

The UV-Vis spectral analysis was measured using Shimadzu UV-2400 PC series spectrophotometer. It involved the absorption of electromagnetic radiation from 200-400 nm range and subsequent excitation of electrons to higher energy states. It was equipped with

1 cm quartz cell and a slit width of 2.0 nm. The UV-Vis spectra of PCMC were recorded in methanol solution at ambient temperature. This analysis was performed to evaluate the effect of biofield treatment on the structural property of PCMC sample. The UV-Vis spectroscopy provided the preliminary information related to the skeleton of chemical structure and possible arrangement of functional groups. With UV-Vis spectroscopy, it was possible to investigate electron transfers between orbitals or bands of atoms, ions and molecules existing in the gaseous, liquid and solid phase [28].

GC-MS analysis

The Gas chromatography-Mass spectrometry (GC-MS) analysis was performed on Perkin Elmer/auto system XL with Turbo Mass, USA, having detection limit up to 1 pictogram. For GC-MS analysis the treated sample was further divided into four parts as T1, T2, T3 and T4. The GC-MS data was obtained in the form of % abundance *vs.* mass to charge ratio (*m/z*), which is known as mass spectrum. The isotopic ratio of $\delta^{13}C$, $\delta^{18}O$ and $\delta^{37}Cl$ were expressed by their deviation in observed value as compared to the control sample. PM was considered as primary molecule and molecular ion peak of PCMC molecule is known as (PM+1) peak which comes from the molecules that contain a ^{13}C atom in place of a ^{12}C. The percent change in isotopic ratio of $\delta^{13}C$ i.e., from observed value was computed from the following formula:

$$\text{percent change } \delta^{13}\text{C isotopic ratio} = \frac{R_{\text{Treated}} - R_{\text{Control}}}{R_{\text{Control}}} \times 100 \quad (1)$$

Where, R_{Treated} and R_{Control} were ratio of intensity at *m/z*=143 to *m/z*=142 in mass spectra of treated and control samples, respectively. Similarly, the percent change in isotopic ratio of $\delta^{18}O$ and $\delta^{37}Cl$ were computed.

Results and Discussion

X-ray diffraction

X-ray diffraction analysis was conducted to study the crystalline nature of the control and treated sample of PCMC. X-ray diffractogram of control and treated samples of PCMC are shown in Figure 2. The X-ray diffractogram of control PCMC showed intense crystalline peaks at 2θ equals to 14.29°, 14.48°, 16.28°, 24.61°, 26.93°, 27.22°, and 31.83°. The intense peaks indicated the crystalline nature of PCMC. However, the X-ray diffractogram of treated PCMC showed the crystalline peaks at 2θ equals to 14.12°, 14.27°, 15.71°, and 31.90°. The peak at 2θ equals to 15.71° showed high intensity as compared to control which indicated that crystallinity of treated PCMC sample increased along the corresponding plane as compared to control. It was reported that the crystal structure of PCMC was characterized by two independent molecules which were different from each other in terms of O-H—O, C-H—π and π-π interactions. These non-covalent interactions emphasize the different spatial environment for both types of molecules. Besides, the molecules of PCMC possess different symmetrical positions due to these intermolecular bonding [29]. It is presumed that biofield energy may be absorbed by the treated PCMC molecules that may lead to breaking of these intermolecular interactions. Due to this, the PCMC molecules may form a symmetrical crystalline long range pattern which further leads to increasing the symmetry of PCMC molecules. Further, the intensity of other peaks decreased in treated sample as compared to control. Hence the other possibility for increased intensity of peak at 2θ equals to 15.71° is that the molecules of neighbouring plane may orient themselves in this plane after biofield treatment. Besides, the crystallite size was found to

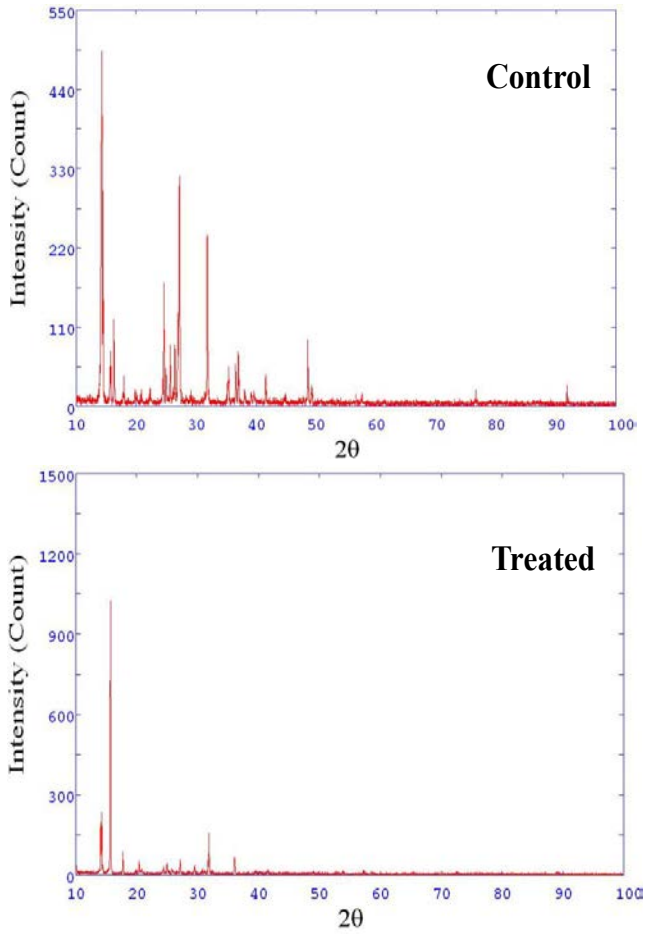

Figure 2: X-ray diffractogram (XRD) of control and treated samples of *p*-chloro-*m*-cresol.

be 86.58 and 97.58 nm in control and treated PCMC, respectively. The crystallite size was increased by 12.71% in treated PCMC as compared to control (Figure 3). It is hypothesized that biofield energy might induce the movement of crystallite boundaries that causes growth of crystals and hence increased crystallite size [30,31].

Surface area analysis

The surface area of control and treated samples of PCMC were investigated using BET method. The control sample showed a surface area of 0.109 m^2/g; however, the treated sample of PCMC showed a surface area of 0.163 m^2/g. The increase in surface area was 49.54% in the treated PCMC sample as compared to control (Figure 3). Our group previously reported that biofield treatment probably increase the surface area due to reduction in particle size through high internal strain and energy milling [30]. Hence, it might be the reason for increase in surface area of treated PCMC as compared to control sample. As it was reported that PCMC is slightly soluble in water hence, the treated sample with increased surface area can help to increase the solubility of PCMC and may solve the solubility problem during manufacturing of several pharmaceutical products.

Thermal studies

DSC analysis: DSC was used to determine the latent heat of fusion

(ΔH) and melting temperature in control and treated sample of PCMC. The DSC analysis results of control and treated samples of PCMC are presented in Table 1. In a solid, the amount of energy required to change the phase from solid to liquid is known as the latent heat of fusion. The data showed that ΔH was decreased from 134.79 J/g (control) to 99.82 J/g in treated PCMC. It indicated that ΔH was decreased by 25.94% in treated sample as compared to control. It was previously reported that PCMC molecules possess intermolecular interactions [29]. Hence, it is hypothesized that biofield energy was absorbed by PCMC molecules that possibly breaks the intermolecular bonding between O-H····O, C-H····π and π····π bonds. Hence, the treated PCMC sample needs less energy in the form of ΔH to undergo the process of melting. This result was also supported by XRD studies. Previously, our group reported that biofield treatment has altered ΔH in lead and tin powder [32]. Moreover, the melting temperature of treated (66.67°C) sample showed very slight change with respect to control (66.17°C) PCMC sample.

TGA/DTG analysis: Thermogravimetric analysis/derivative thermogravimetry analysis (TGA/DTG) of control and biofield treated samples are summarized in Table 1. TGA thermogram showed that control PCMC sample started losing weight around 145°C (onset) and stopped around 187°C (end set). However, the treated PCMC started losing weight around 130°C (onset) and terminated around 197°C (end set). It indicated that onset temperature of treated PCMC decreased by 10.34% as compared to control. Besides, DTG thermogram data showed that T_{max} in control and treated sample were approximately same i.e., 161.49°C and 161.29°C, respectively. The result of TGA/DTG analysis did not revealed any significant change except the onset temperature which was slightly decreased in treated sample as compared to control.

Spectroscopic studies

FT-IR analysis: The FT-IR spectra of control and treated (T1 and T2) samples are shown in Figure 4. The spectra showed characteristic vibrational frequencies as follows:

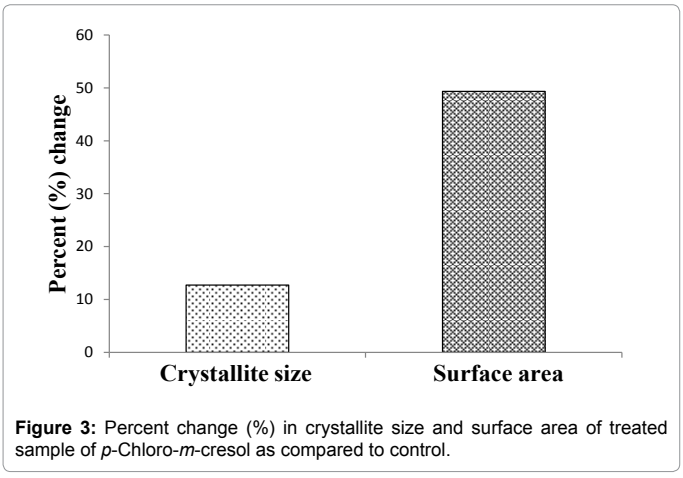

Figure 3: Percent change (%) in crystallite size and surface area of treated sample of *p*-Chloro-*m*-cresol as compared to control.

Parameter	Control	Treated
Latent heat of fusion ΔH (J/g)	134.78	99.82
Melting point (ºC)	66.17	66.67
Onset temperature (ºC)	145	130
T_{max} (ºC)	161.49	161.29

Table 1: Thermal analysis of control and treated samples of p-chloro-m-cresol. Tmax: Temperature at which maximum weight loss occur; PCMC: p-Chloro-m-cresol.

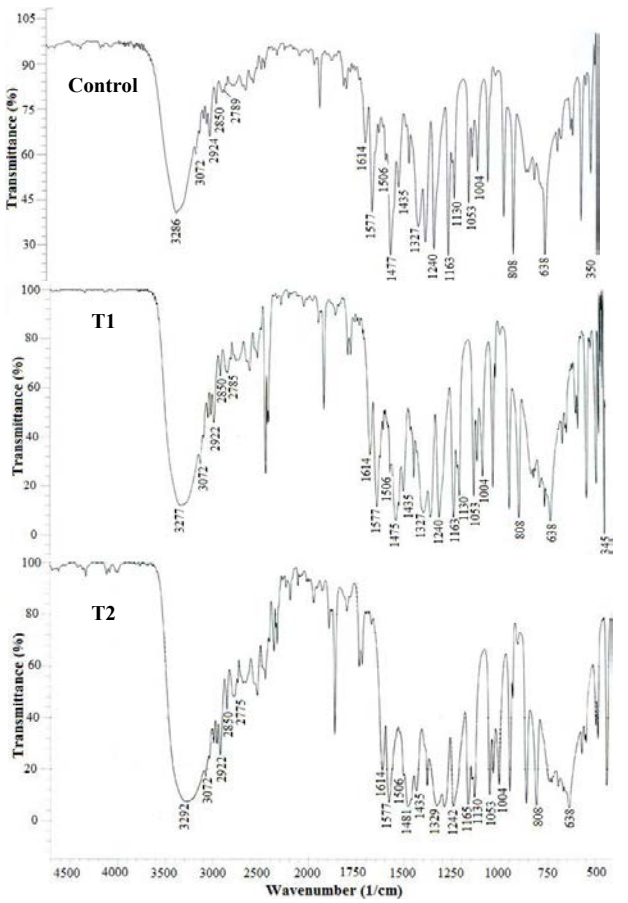

Figure 4: FT-IR spectra of control and treated (T1 and T2) samples of *p*-chloro-*m*-cresol.

Carbon-hydrogen vibrations

The frequency of C-H stretching was observed at 3072 cm^{-1} in all three samples i.e., control, T1 and T2. The C-H in-plane bending vibrations lie in the region of 1000-1300 cm^{-1} which were observed at 1163, 1130 and 1053 cm^{-1} in control and T1 sample whereas, at 1165, 1130 and 1053 cm^{-1} in T2 sample. The C-H out-of-plane bending vibrations appeared at 808 cm^{-1} in all three samples i.e., control, T1 and T2.

Oxygen-hydrogen vibrations

In the present study the O-H stretching vibration was observed at 3286 cm^{-1} in control sample, whereas at 3277 and 3292 cm^{-1} in T1 and T2 samples respectively. The peak due to O-H in-plane bending vibrations was observed at 1327 cm^{-1} in control and T1 sample and at 1329 cm^{-1} in T2 sample.

C-O group vibration

The most important peak due to C-O stretching mode appeared at 1240 cm^{-1} in control and T1 sample and at 1242 cm^{-1} in T2 sample. This mode can be described as coupled vibrations, involving C-H stretch along with aromatic ring vibration.

Methyl group (CH_3) vibration

The PCMC possess a CH_3 group in the third position of the ring. The infrared band with sharp peaks found at 2924, 2850 and 2789 cm^{-1}

in control sample, at 2922, 2850 and 2785 cm^{-1} in T1 and at 2922, 2850 and 2785 cm^{-1} in T2 samples were assigned to CH_3 stretching. The methyl deformation modes which included in-plane, out-of-plane and rocking modes were observed at 1435, 1506 and 1004 cm^{-1} in all three samples i.e., controls, T1 and T2.

Ring vibrations

In the present study, the peaks observed at 1614, 1577 and 1477 cm^{-1} in control have been assigned to C-C stretching vibrations. In T1, the peaks appeared at 1614, 1577 and 1475 cm^{-1} whereas in T2, these peaks were appeared at 1614, 1577 and 1481 cm^{-1}.

C-Cl vibrations

In FT-IR spectra, the strong band at 638 cm^{-1} was assigned to C-Cl stretching vibration in all three samples i.e., control, T1 and T2. The C-Cl in-plane bending and out-of-plane bending vibrations appeared below 350 cm^{-1} which were not observed in spectra.

The overall analysis was supported from literature data [33] and showed that there was no significant difference between observed frequencies of control and treated (T1 and T2) samples. Hence, it shows that biofield treatment might not induce any changes at bonding level.

UV-Vis spectroscopic analysis

The UV spectra of control and treated samples (T1 and T2) of PCMC are shown in Figure 5. The UV spectrum of control sample showed absorption peaks at λ_{max} equals to 206 and 247 nm. It was also reported that PCMC may undergone the process of photolysis. It happens because in the structure of PCMC, the chlorine and methyl substituent occupy adjacent positions in aromatic ring which could be a possible reason for photolytically induced interaction between these groups. Hence, it is possible that intramolecular photolysis could produce a mixture of intermediates [34], which might be responsible for absorbing light and showed peak at wavelength 247 nm. However the biofield treated sample T1 showed absorption peaks at 204, 228 and 282 nm and T2 showed peaks at 203, 228 and 282 nm. Hence, it is hypothesized that biofield treatment might reduce the photo degradation of PCMC that make it more suitable for use in various pharmaceutical preparations.

GC-MS analysis

The mass spectra of control and treated (T1, T2, T3, and T4) samples of PCMC (C_7H_7ClO) are shown in Figure 6a, 6b and 6c. The mass spectra of control and treated samples showed different intensities. Mass spectra showed that base peak was observed at *m/z*=107 in control sample (Figure 6a). The treated samples i.e., T1, T3 and T4 also showed the base peak at *m/z*=107 whereas in T2 sample, the base peak was found at *m/z*=142. Furthermore, the intense peaks with different mass to charge ratio (*m/z*), of possible molecular ions are illustrated in Table 2. It indicated that peak at *m/z*=107 and *m/z*=142 in control and treated samples (T1, T2, T3, and T4) were due to $^{12}C_7H_6OH^+$ and $^{12}C_7H_6ClO^+$ respectively. Computed result of carbon isotopic ratio ($\delta^{13}C$) using equation (1) is shown in Table 3 and Figure 7. It showed that the percent change in $\delta^{13}C$ of treated samples i.e., T1, T2, T3, and T4 were found as -4.10, 128.47, 204.85 and -6.36%, respectively as compared to control sample. The significant change was observed in T2 and T3 samples which suggest that the ^{12}C atoms in T2 and T3, probably transformed into ^{13}C by capturing one neutron thereby increased ^{13}C. Similarly, the computed result of oxygen and chlorine isotopic ratio ($\delta^{18}O$ and $\delta^{37}Cl$) is shown in Table 4 and Figure 8. It showed that percent changes in $\delta^{18}O$ and $\delta^{37}Cl$ of treated samples i.e., T1, T2, T3, and T4 were found as -3.25, 128.44, 142.28 and -3.67%, respectively as compared to control sample. The significant change found in T2 and T3 samples suggest the probable conversion of $^{16}O \rightarrow ^{18}O$ and $^{35}Cl \rightarrow ^{37}Cl$ by capturing two neutrons after biofield treatment. The inter-conversion of these isotopes can be possible if a nuclear level reaction including the neutron and proton occurred after biofield energy treatment. Thus, it is assumed that biofield treatment possibly induced the nuclear level reactions through its energy, which may lead to alter the isotopic ratio of $\delta^{13}C$, $\delta^{18}O$ and $\delta^{37}Cl$ in treated PCMC. Besides, it is well known that various isotopes of an element have similar charge but different masses which means that heavier isotope has greater mass as compared to lighter one. Also, greater the mass of molecule means more energy is needed to break the bond. Hence, it revealed that the treated samples (T2 and T3) might be more stable, since the higher isotopes of carbon, oxygen and chlorine are more abundant in these samples as compared to control [35,36].

Thus, GCMS data suggest that biofield energy treatment has significantly altered the isotopic ratio of $\delta^{13}C$, $\delta^{18}O$ and $\delta^{37}Cl$ in treated PCMC samples which make them more stable as compared to control sample. The impact of biofield energy treatment was also analysed in some other similar structured compounds *viz.* thymol, menthol, and resorcinol and it was reported that biofield energy has significantly altered the physical, thermal and spectral properties of those compounds [37,38].

Conclusion

The XRD study showed the increase in crystallinity as well as crystallite size (12.71%) in treated sample as compared to control. The

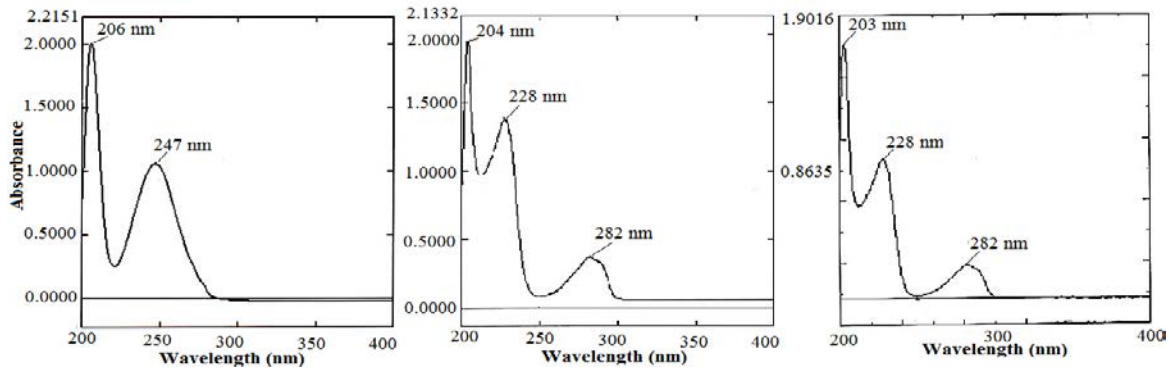

Figure 5: UV-Vis spectra of control and treated (T1 and T2) samples of *p*-chloro-*m*-cresol.

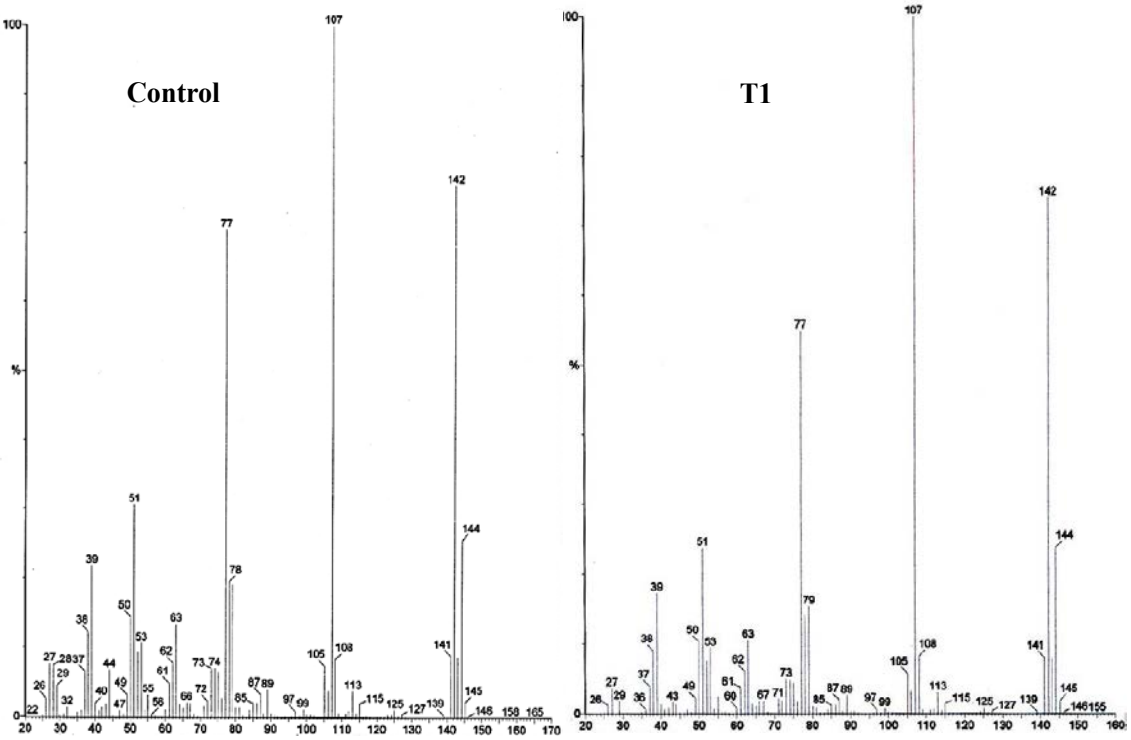

Figure 6a: GC-MS spectra of control and treated (T1) samples of *p*-chloro-*m*-cresol.

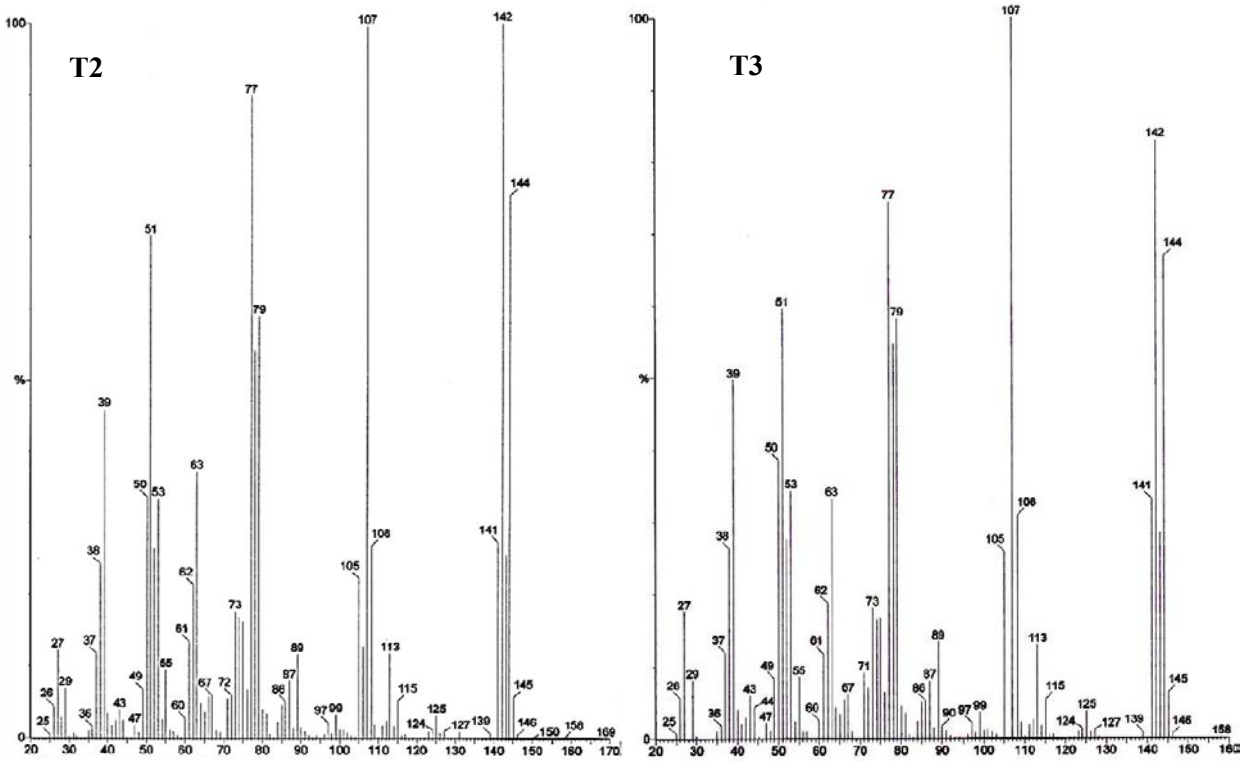

Figure 6b: GC-MS spectra of treated (T2 and T3) samples of p-chloro-m-cresol.

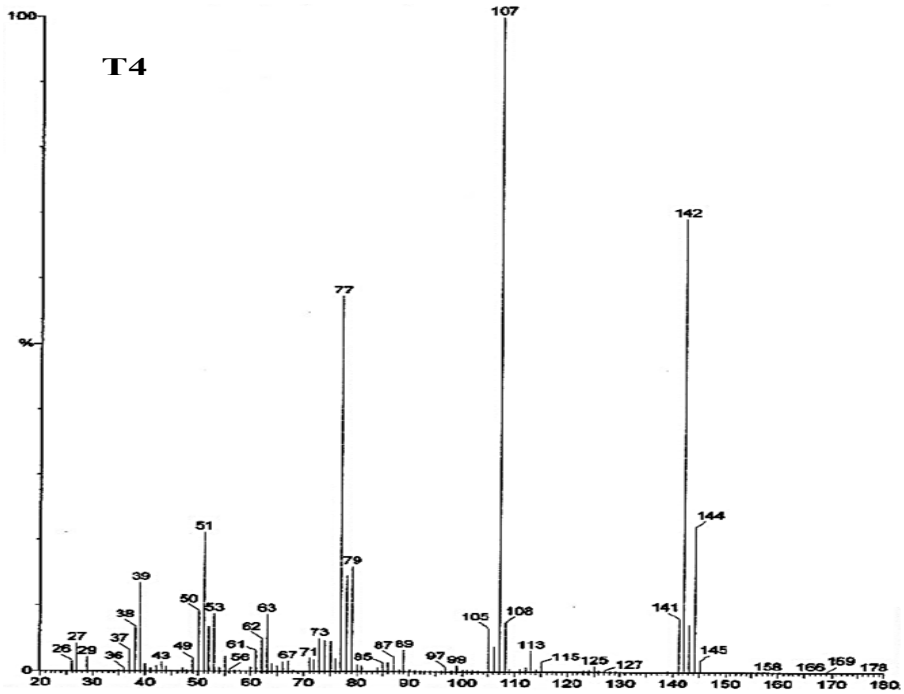

Figure 6c: GC-MS spectrum of treated (T4) sample of *p*-chloro-*m*-cresol.

Ratio *m/z*	Possible detected molecules
142	$^{12}C_7H_6ClO^+$
107	$^{12}C_7H_7O^+$
77	$^{12}C_6H_5^+$
51	$^{12}C_4H_3^+$
39	$^{12}C_3H_3^+$

Table 2: Identification of peaks in mass spectra of p-chloro-m-cresol. PCMC: p-Chloro-m-cresol.

Samples	Parameters	
	$\delta^{13}C$ isotopic ratio Observed	Percent change with respect to control
Control	11.243	-
T1	10.782	-4.105
T2	25.69	128.477
T3	34.277	204.854
T4	10.528	-6.362

Table 3: $\delta^{13}C$ isotopic ratio analysis result of *p*-chloro-*m*-cresol.

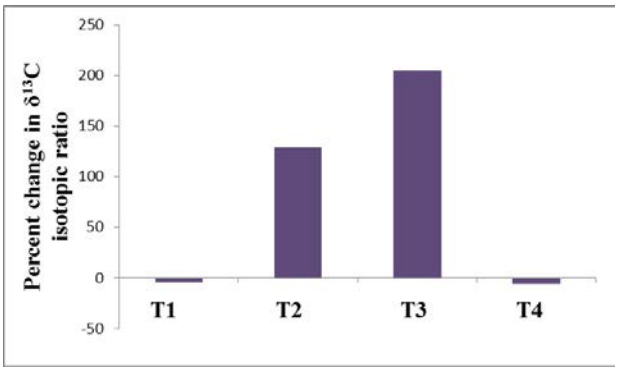

Figure 7: Percent change in carbon isotopic ratio (δ13C) in treated samples as compared to control.

Samples	Parameters	
	$\delta^{18}O$ and $\delta^{37}Cl$ isotopic ratio Observed	Percent change with respect to control
Control	33.212	-
T1	32.130	-3.255
T2	75.87	128.441
T3	80.467	142.285
T4	31.990	-3.678

Table 4: $\delta^{18}O$ and $\delta^{37}Cl$ isotopic ratio in control and treated samples of *p*-chloro-*m*-cresol.

increase in crystallinity might be due to breaking of intermolecular bonding after biofield treatment that results in more symmetrical alignment of PCMC molecules. The surface area analysis also revealed 49.54% increase in surface area which might be helpful to increase the solubility of treated PCMC as compared to control sample. The DSC analysis of treated sample showed 25.94% decrease in ΔH value as compared to control, which probably occurred due to absence of intermolecular bonding in biofield treated sample as reported in XRD studies. The UV-Vis spectroscopic study revealed that biofield treatment probably reduces the photo degradation of PCMC sample. On the other hand, the GC-MS data revealed the alteration in the isotopic ratio of $\delta^{13}C$, $\delta^{18}O$ and $\delta^{37}Cl$ and increase in abundance of $\delta^{13}C$, $\delta^{18}O$ and $\delta^{37}Cl$ in biofield treated samples as compared to control. The increased abundance of heavier isotopes suggests the increased stability of treated samples as compared to control. In spite of wide applications of PCMC, its effectiveness was reduced in presence of oils, fats or non-ionic surfactants. Also it faces solubility problem in water and can undergo the process of photo degradation which causes stability issues. Hence, on the basis of above study results, it is concluded that

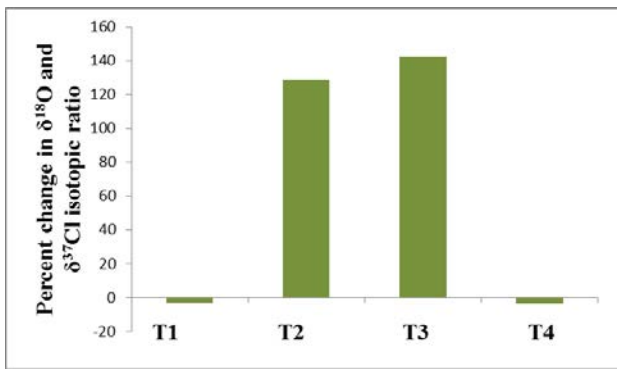

Figure 8: Percent change in $\delta^{18}O$ and $\delta^{37}Cl$ isotopic ratio in treated samples as compared to control.

biofield treatment has significantly altered the physical, thermal and spectroscopic properties of PCMC which could make it more suitable with respect to increased solubility and stability profile along with reduction in problem of photo degradation.

Acknowledgements

The authors would like to acknowledge the whole team of Sophisticated Analytical Instrument Facility (SAIF), Nagpur, Indian Rubber Manufacturers Research Association (IRMRA), Thane and MGV Pharmacy College, Nashik for providing the instrumental facility. We are very grateful for the support of Trivedi Science, Trivedi Master Wellness and Trivedi Testimonials in this research work.

References

1. Abdelaziz AA, el-Nakeeb MA (1987) Sporicidal activity of local anaesthetics and their binary combinations with preservatives. J Basic Microbiol 27: 403-410.
2. Dooms-Goossens A, Degreef H, Vanhee J, Kerkhofs L, Chrispeels MT (1981) Chlorocresol and chloracetamide: allergens in medications, glues, and cosmetics. Contact Dermatitis 7: 51-52.
3. Oneil MJ (2006) The Merck Index - An encyclopedia of chemicals, drugs, and biologicals. 14th edn. Merck and Co. Inc., USA.
4. Wawley GG (1981) The condensed chemical dictionary. 10th edn. Van Nostrand Reinhold Company, New York, USA.
5. Grant WM (1987) Toxicology of the eye. 3rd edn. Charles C, Thomas Publisher, Springerfield, Illinois.
6. Andersen A (2006) Final report on the safety assessment of sodium p-chloro-m-cresol, p-chloro-m-cresol, chloro thymol, mixed cresols, m-cresol, o-cresol, p-cresol, isopropyl cresols, thymol, o-cymen-5-ol, and carvacrol. Int J Toxicol 25 Suppl 1: 29-127.
7. Rossoff IS (1974) Handbook of veterinary drugs. Springer publishing company, New York.
8. Zorzato F, Scutari E, Tegazzin V, Clementi E, Treves S (1993) Chlorocresol: an activator of ryanodine receptor-mediated Ca^{2+} release. Mol Pharmacol 44: 1192-1201.
9. Pharmaceutical Society of Great Britain (1979) The Pharmaceutical Codex. 11th edn. Pharmaceutical Press, London, UK.
10. Uchida S, Iha T, Yamaoka K, Nitta K, Sugano H (2012) Effect of biofield therapy in the human brain. J Altern Complement Med 18: 875-879.
11. Giasson M, Bouchard L (1998) Effect of therapeutic touch on the well-being of persons with terminal cancer. J Holist Nurs 16: 383-398.
12. Peck SD (1998) The efficacy of therapeutic touch for improving functional ability in elders with degenerative arthritis. Nurs Sci Q 11: 123-132.
13. Rivera-Ruiz M, Cajavilca C, Varon J (2008) Einthoven's string galvanometer: the first electrocardiograph. Tex Heart Inst J 35: 174-178.
14. Rubik B (2002) The biofield hypothesis: its biophysical basis and role in medicine. J Altern Complement Med 8: 703-717.
15. Garland SN, Valentine D, Desai K, Li S, Langer C, et al. (2013) Complementary and alternative medicine use and benefit finding among cancer patients. J Altern Complement Med 19: 876-881.
16. Saad M, Medeiros RD (2012) Distant healing by the supposed vital energy- Scientific bases. Complementary Therapies for the Contemporary Healthcare. USA.
17. Shinde V, Sances F, Patil S, Spence A (2012) Impact of biofield treatment on growth and yield of lettuce and tomato. Aust J Basic Appl Sci 6: 100-105.
18. Sances F, Flora E, Patil S, Spence A, Shinde V (2013) Impact of biofield treatment on ginseng and organic blueberry yield. Agrivita J Agric Sci 35: 22-29.
19. Lenssen AW (2013) Biofield and fungicide seed treatment influences on soybean productivity, seed quality and weed community. Agricultural Journal 8: 138-143.
20. Nayak G, Altekar N (2015) Effect of biofield treatment on plant growth and adaptation. J Environ Health Sci 1: 1-9.
21. Patil SA, Nayak GB, Barve SS, Tembe RP, Khan RR (2012) Impact of biofield treatment on growth and anatomical characteristics of *Pogostemon cablin* (Benth.). Biotechnology 11: 154-162.
22. Trivedi MK, Bhardwaj Y, Patil S, Shettigar H, Bulbule, A (2009) Impact of an external energy on *Enterococcus faecalis* [ATCC-51299] in relation to antibiotic susceptibility and biochemical reactions-an experimental study. J Accord Integr Med 5: 119-130.
23. Trivedi MK, Patil S (2008) Impact of an external energy on *Staphylococcus epidermis* [ATCC-13518] in relation to antibiotic susceptibility and biochemical reactions-an experimental study. J Accord Integr Med 4: 230-235.
24. Trivedi MK, Patil S (2008) Impact of an external energy on *Yersinia enterocolitica* [ATCC-23715] in relation to antibiotic susceptibility and biochemical reactions: An experimental study. Internet J Alternat Med 6: 13.
25. Trivedi MK, Tallapragada RR (2008) A transcendental to changing metal powder characteristics. Met Powder Rep 63: 22-28.
26. Dabhade VV, Tallapragada RR, Trivedi MK (2009) Effect of external energy on atomic, crystalline and powder characteristics of antimony and bismuth powders. Bull Mater Sci 32: 471-479.
27. Trivedi MK, Patil S, Shettigar H, Singh R, Jana S (2015) An impact of biofield treatment on spectroscopic characterization of pharmaceutical compounds. Mod Chem appl 3: 159.
28. Pavia DL, Lampman GM, Kriz GS (2001) Introduction to spectroscopy. 3rd edn, Thomson Learning, Singapore.
29. Cox PJ (2003) Supramolecular structures of 2-chloro-5-methylphenol and 4-chloro-3-methylphenol (chlorocresol). Acta Crystallogr C 59: o533-536.
30. Trivedi MK, Nayak G, Tallapragada RM, Patil S, Latiyal O, et al. (2015) Effect of biofield treatment on structural and morphological properties of silicon carbide. J Powder Metall Min 4: 132.
31. Trivedi MK, Nayak G, Tallapragada RM, Patil S, Latiyal O, et al. (2015) Influence of biofield treatment on physical, structural and spectral properties of boron nitride. J Material Sci Eng 4: 181.
32. Trivedi MK, Patil S, Tallapragada RM (2013) Effect of biofield treatment on the physical and thermal characteristics of silicon, tin and lead powders. J Material Sci Eng 2: 125.
33. Krishna Kumar V, Kumar M, Prabavathi N, Mathammal R (2012) Molecular structure, spectroscopic studies (FTIR, FT-Raman and NMR) and HOMO-LUMO analysis of 6-chloro-o-cresol and 4-chloro-3-methyl phenol by density functional theoretical study. Spectrochim Acta A Mol Biomol Spectrosc 97: 144-154.
34. Callahan MA (1979) Water-related environmental fate of 129 priority pollutants. Office of Water and Waste Management, US Environmental Protection Agency, USA.
35. Kohen A, Limbach HH (2005) Isotope Effects in Chemistry and Biology. CRC press, USA.
36. Califano S (1976) Vibrational States. Wiley-VCH, New York, USA.
37. Trivedi MK, Patil S, Mishra RK, Jana S (2015) Structural and Physical Properties of Biofield Treated Thymol and Menthol. J Mol Pharm Org Process Res 3: 127.
38. Trivedi MK, Branton A, Trivedi D, Nayak G, Singh R, et al. (2015) Characterisation of Physical, Spectral and Thermal Properties of Biofield treated Resorcinol. Organic Chem Curr Res 4: 146.